NJC

PAPER

View Article Online
View Journal | View Issue

Cite this: *New J. Chem.*, 2015, 39, 4265

Influence of noncovalent interactions on the structures of metal–organic hybrids based on a $[VO_2(2,6\text{-pydc})]^-$ tecton with cations of imidazole, pyridine and its derivatives†

Tanja Koleša-Dobravc,[ab] Anton Meden[ab] and Franc Perdih*[ab]

Seven different dioxido(pyridine-2,6-dicarboxylato)vanadate(v) compounds with pyridinium (Hpy^+) (**1**·2H_2O and **1**), 2-hydroxypyridinium (H2pyon$^+$) (**2**·H_2O), 4-aminopyridinium (H4apy$^+$) (**3**·H_2O and **3**), 4-(dimethylamino)pyridinium ($Hdmap^+$) (**4**·H_2O) and imidazolium ($Himd^+$) (**5**) cations have been prepared *via* different pathways starting either from pyridine-2,6-dicarboxylic acid or its esters, and were structurally characterized by single-crystal X-ray diffraction. The vanadium metal center in dioxido(pyridine-2,6-dicarboxylato)vanadate(v) anion is pentacoordinated in all of the compounds: having two oxido oxygen atoms in a mutual *cis* position and a tridentate pyridine-2,6-dicarboxylic ligand. Study of hydrogen bonds and weak interactions in the compounds revealed the relationship between the type of cation and the hydrogen bonding network in the compounds. While in **1**·2H_2O, **2**·H_2O and **4**·H_2O a one-dimensional (band, pillar or chain) hydrogen bonding network *via* N/O–H···O bonds is preferred, anhydrous **3** and **3**·H_2O favor a two-dimensional hydrogen-bonded framework, and the $Himd^+$ cation facilitates a three-dimensional hydrogen bonding in **5**. The unique vanadium coordination environment with two easily accessible oxido oxygen atoms of the VO_2^+ unit is suitable for the construction of non-covalent metal–organic hybrids. In **2**·H_2O, **3**·H_2O, **4**·H_2O and **5** both oxido oxygen atoms of the VO_2^+ unit participate as acceptors, however, in **1**·2H_2O and **3** only one oxido oxygen atom is involved in classical hydrogen bonding. Besides N/O–H···O hydrogen bonding, also other weak non-covalent interactions, such as C–H···O, π···π and C–H···π interactions, play an important role in stabilizing the crystal lattices.

Received (in Montpellier, France) 20th January 2015,
Accepted 16th March 2015

DOI: 10.1039/c5nj00164a

www.rsc.org/njc

Introduction

The self-assembly of tectons into extended network structures is the core of supramolecular chemistry and crystal engineering. Metal–organic hybrids and especially metal–organic frameworks are currently an extremely important topic and an active area of research because of their intriguing architectures and topologies,[1] as well as due to their potential application in catalysis,[2] chemical separation processes,[3] gas storage,[4] magnetism[5] and as sensors.[6]

Metal–organic hybrids can be assembled by a covalent approach using bridging ligands or by a non-covalent approach using hydrogen bonding and other weak interactions. The covalent approach is primarily based on strong coordinate bonds connecting metal cations and organic ligands into robust polymeric structures. Different kinds of these materials have been designed with special attention dedicated to the geometry of the metal ions as well as flexibility, bridging potential and coordination preferences of different organic linkers.[1] In the non-covalent approach much weaker forces, such as hydrogen bonding, C–H···π/F interactions, π···π stacking, and halogen bonding, are employed. Although weak by nature multiple non-covalent forces can adjust the dimensionality and enable new topologies to arise. Therefore, the desired functions of supramolecular assemblies can be achieved.[7–10] Among non-covalent interactions the hydrogen bonding is a particularly powerful building motif used in crystal engineering since it provides unique directionality and can be easily introduced into structures. There exists a great variety of hydrogen bonding donors–acceptors and their numbers can be varied through simple design, thus making them a particularly good choice for the construction of self-assemblies. With this approach a wide variety of mononuclear, dinuclear and polynuclear coordination compounds/ions can be assembled into desirable motifs. Multiple weak non-covalent interactions can even control the topology of metal–organic frameworks[11] as well as the coordination geometry.[12]

[a] *Faculty of Chemistry and Chemical Technology, University of Ljubljana, Večna pot 113, P. O. Box 537, SI-1000 Ljubljana, Slovenia*
[b] *CO EN–FIST, Trg Osvobodilne fronte 13, SI-1000 Ljubljana, Slovenia. E-mail: franc.perdih@fkkt.uni-lj.si*

† Electronic supplementary information (ESI) available. CCDC 1030256–1030262. For ESI and crystallographic data in CIF or other electronic format see DOI: 10.1039/c5nj00164a

Although great efforts have been made toward the understanding of the assembly process, rational control in the construction of supramolecular structures of complexes is still a challenging task. For the construction of a desired framework and functionality, it is important to control and understand the factors, such as counterions, solvents, temperature and pH value, that tend to influence the structural prediction on the assembly of the final coordination frameworks and govern the crystal growth and the stability of the overall crystals.[1b,13] Among the above factors, it has been demonstrated that counterions have a significant effect on the formation of the product. Different coordination abilities, sizes, and geometries of anions have a great influence on the structural assembly and importantly influence the prediction of the overall supramolecular architectures of coordination compounds.[1b,14] Cations can also have a significant influence on the crystal architecture. "Naked" alkali cations are useful tectons due to their different sizes and polarisability, while in the case of NH_4^+ and hydrated cations, besides their size and charge, the hydrogen bonding capacity can enable the formation of high-dimensional frameworks.[15] Diverse effects can be introduced by organic cations, most commonly protonated cationic amines and pyridines. Organic cations can be varied through simple design and diverse functionalities can be combined. Coulombic interactions are a principal force for cation–anion arrangements in supramolecular structures.[16] However, protonated organic cations can also act as multi-hydrogen bond donors as well as acceptors and thus easily adjust the topologies *via* additional non-covalent interactions. Charge-assisted or ionic hydrogen bonds are in general stronger hydrogen bonds since ionic charge on a donor or an acceptor enhances the hydrogen bond strength.[17] Furthermore, employing organic cations enables introduction of additional weak non-covalent interactions, such as π···π stacking, C–H···π interactions and halogen bonding.[18]

Recently, the use of bioactive framework materials (BioMOFs) has gained considerable attention in biology and medicine. This has stimulated the search for new types of bioactive organic linkers capable of ligating biorelevant metal ions for the design of functional materials.[19,20] Multidentate pyridinedicarboxylato ligands ($pydc^{2-}$) have been widely used in recent years for the construction of organic–inorganic hybrid materials. Because they possess diverse coordination abilities, flexibilities and various bridging modes, supramolecular networks of high structural stability have been assembled either *via* coordination bonds, hydrogen bonds and/or aromatic interactions.[21] Some biological activities of multidentate pyridinedicarboxylate have already been demonstrated, such as antimicrobial activity and DNA cleavage.[22]

The field of vanadium metal–organic hybrids started to grow considerably since the discovery of MIL-26 and MIL-47 in the early period of the last decade.[23] We are especially interested in extending the knowledge of self-assembly of vanadium compounds because of their potential therapeutic application such as insulin-enhancing agents. An important advantage of vanadium compounds in the treatment of diabetes mellitus compared to insulin is the possibility of oral administration.[24]

In this study new supramolecular networks built by pyridine-2,6-dicarboxylic acid (2,6-H_2pydc, dipicolinic acid) were generated containing various organic cations in order to evaluate the role of cations and anions in crystal engineering. Compared with other transition metal cations, vanadium ions possess distinctly different properties and coordination modes, which play key roles in the formation of both coordination structures and packing structures of complexes. For example, vanadium(v) compounds usually contain a typical *cis*-VO_2^+ moiety with an overall five- or six-coordination. The VO_2^+ as well as VO^{2+} group can also participate in weak V=O···C interactions as pointed out recently.[25] In the studied $[VO_2(2,6\text{-pydc})]^-$ systems the VO_2^+ moiety is additionally coordinated by one tridentate 2,6-$pydc^{2-}$ ligand forming pentacoordinated geometry. While oxygen atoms being part of the anion allow the formation of numerous hydrogen bonds, the aromatic pyridine ring of 2,6-$pydc^{2-}$ ligand enables additional π···π stacking interactions.

Experimental section

Materials and physical measurements

Reagents and chemicals were purchased as reagent grade from commercial sources and were used without any further purification. Diethyl pyridine-2,6-dicarboxylate ester was prepared according to a published procedure.[26] Infrared (IR) spectra (4000–600 cm^{-1}) of the samples were recorded using a Perkin-Elmer Spectrum 100, equipped with a Specac Golden Gate Diamond ATR as a solid sample support. Elemental (C, H, N) analysis was performed using a Perkin-Elmer 2400 Series II CHNS/O Elemental Analyzer. Powder X-ray diffraction patterns were collected on a Siemens D-5000 diffractometer with θ–2θ Bragg–Brentano geometry operating using Cu-K_α radiation.

Preparation

Procedure A. General procedure for the synthesis of V(v) complexes 1·2H_2O and 2·H_2O starting from pyridine-2,6-dicarboxylic acid. To a mixture of sodium metavanadate (0.50 mmol, 97 mg) and pyridine-2,6-dicarboxylic acid (0.50 mmol, 84 mg) water (3 mL) was added and stirred for 10 min at room temperature to yield a yellow solution. Separately, py or 2hypy (0.50 mmol) was dissolved in a mixture of water (2 mL) and hydrochloric acid (2 M, 0.25 mL) and then slowly added to the vanadium solution. The mixture was stirred at 70 °C for 15 min, filtered and stored under room conditions. The solution was allowed to evaporate slowly at room temperature for a week, and crystals suitable for single crystal X-ray diffraction analysis were obtained.

Procedure B. General procedure for the synthesis of V(v) complexes 3·H_2O, 4·H_2O and 5 starting from pyridine-2,6-dicarboxylic acid. Ammonium metavanadate (0.50 mmol, 59 mg) and pyridine-2,6-dicarboxylic acid (0.50 mmol, 84 mg) were dissolved in water (3 mL). To the yellow solution a solid nitrogen base (0.50 mmol) and methanol (3 mL) were added. The mixture was stirred at 70 °C for 30 min, filtered and stored under room conditions. The solution was allowed to evaporate

slowly at room temperature for a few days, and crystals suitable for single crystal X-ray diffraction analysis were obtained.

Procedure C. General procedure for the synthesis of V(v) complexes 1, 3, 4·H_2O and 5 starting from diethyl pyridine-2,6-dicarboxylate ester. A mixture of diethyl pyridine-2-dicarboxylate (112 mg, 0.50 mmol) and sodium hydroxide (20 mg, 0.50 mmol) in ethanol (6 mL) was added dropwise to an ethanol (2 mL) solution of $VOSO_4·5H_2O$ (63 mg, 0.25 mmol). After addition of a nitrogen base (0.25 mmol) and toluene (1 mL), the green mixture was stirred at 50 °C for 15 min. The solution was cooled to room temperature and filtered. It was allowed to evaporate slowly at room temperature for a few days, and crystals suitable for single crystal X-ray diffraction analysis were obtained.

Procedure D. Procedure for the synthesis of V(v) complex 2·H_2O starting from 6-((pyridin-2-yloxy)carbonyl)pyridine-2-carboxylic acid. A mixture of 6-((pyridin-2-yloxy)carbonyl)pyridine-2-carboxylic acid (49 mg, 0.20 mmol) and sodium acetate trihydrate (27 mg, 0.20 mmol) in methanol (3 mL) was added dropwise to a methanol (2 mL) solution of $VOSO_4·5H_2O$ (25 mg, 0.10 mmol). The resulting yellow to green mixture was stirred at 50 °C for 20 min, and then filtered and stored under room conditions. The solution was allowed to evaporate slowly at room temperature for a few days, and crystals suitable for single crystal X-ray diffraction analysis were obtained.

Synthesis of 6-((pyridin-2-yloxy)carbonyl)pyridine-2-carboxylic acid. Di(pyridin-2-yl) pyridine-2,6-dicarboxylate[27] (773 mg, 2.41 mmol) was dissolved in a methanol/tetrahydrofuran mixture (2 : 1, 30 mL). To the solution KOH (151 mg, 2.69 mmol) in methanol (3 mL) was added in small portions. After stirring overnight at room temperature, water (30 mL) was added and volatile solvents were removed *in vacuo*. The water residue was extracted with dichloromethane (20 mL) and then acidified to pH 2 with 1 M HCl. The aqueous layer was extracted with dichloromethane (5 × 15 mL). Combined organic layers were washed with brine (15 mL) and dried with anhydrous $MgSO_4$. Solvents were removed *in vacuo* yielding a white solid compound. Yield: *m* = 272 mg (46%). ^{1}H NMR ($CDCl_3$, 500 MHz): δ 8.54 (m, 1H, Py-*H*), 8.50 (d, *J* = 7 Hz, 2H, Ar-*H* 2,6-pydc), 8.20 (t, *J* = 7 Hz, 1H, Ar-*H* 2,6-pydc), 7.91 (m, 1H, Py-*H*), 7.35 (m, 1H, Py-*H*), 7.28 (m, 1H, Py-*H*).

Hpy[VO_2(2,6-pydc)]·2H_2O (**1**·2H_2O) was prepared according to procedure A. Yield: *m* = 53 mg (30%), CHN elemental analysis: calculated for monohydrate $C_{12}H_{11}N_2O_7V$ (%): C 41.64, H 3.20, N 8.09; found: C 41.45, H 3.08, N 8.01. IR (ATR, cm^{-1}): 3365m, 3097w, 3066w, 2663br, 2190w, 1685s, 1636m, 1545w, 1484m, 1435w, 1333s, 1252w, 1168m, 1148w, 1078m, 1033w, 946s, 918s, 881m, 850w, 749s, 690m, 677s.

Hpy[VO_2(2,6-pydc)] (**1**) was prepared according to procedure C. Only a few crystals were taken out from the solution and used for X-ray analysis. Other crystals were left in the mother liquid and after a few days, probably due to the incorporation of air moisture, transformed into **1**·2H_2O crystals.

H2pyon[VO_2(2,6-pydc)]·H_2O (**2**·H_2O) was prepared according to procedures A and D. Yield: *m* = 96 mg (53%), CHN elemental analysis: calculated for $C_{12}H_{11}N_2O_8V$ (%): C 39.80, H 3.06, N 7.73; found: C 39.68, H 2.93, N 7.65. IR (ATR, cm^{-1}): 3393m, 3106w, 3093w, 2496br, 2114w, 1695m, 1600s, 1592s, 1552m, 1476w, 1438w, 1386m, 1371m, 1342s, 1263w, 1169w, 1078m, 951s, 925s, 875m, 852w, 779m, 765m, 748s, 679m, 622w.

H4apy[VO_2(2,6-pydc)]·H_2O (**3**·H_2O) was prepared according to procedure B. Yield: *m* = 132 mg (77%), CHN elemental analysis: calculated for anhydrous $C_{12}H_{10}N_3O_6V$ (%): C 42.00, H 2.94, N 12.24; found: C 41.85, H 2.76, N 12.25. IR (ATR, cm^{-1}): 3336w, 3160m, 3084m, 2941s, 2873w, 2071w, 1681m, 1656s, 1636m, 1530s, 1432w, 1337s, 1191w, 1164w, 1077m, 958m, 937w, 916s, 844w, 817m, 753m, 675m.

H4apy[VO_2(2,6-pydc)] (**3**) was prepared according to procedure C. Yield: *m* = 25 mg (29%), CHN elemental analysis: calculated for $C_{12}H_{10}N_3O_6V$ (%): C 42.00, H 2.94, N 12.24; found: C 42.15, H 2.61, N 12.22. IR (ATR, cm^{-1}): 3336w, 3160m, 3084m, 2941s, 2873w, 2071w, 1681m, 1656s, 1636m, 1530s, 1432w, 1337s, 1191w, 1164w, 1077m, 958m, 937w, 916s, 844w, 817m, 753m, 675m.

Hdmap[VO_2(2,6-pydc)]·H_2O (**4**·H_2O) was prepared according to procedures B and C. Yield: *m* = 140 mg (72%), CHN elemental analysis: calculated for $C_{14}H_{16}N_3O_7V$ (%): C 43.31, H 3.89, N 10.82; found: C 43.10, H 3.87, N 10.78. IR (ATR, cm^{-1}): 3508br, 3222w, 3093w, 2964w, 1681s, 1643m, 1632m, 1602w, 1568m, 1408w, 1334s, 1219m, 1066s, 944s, 922m, 818m, 752m, 744m, 674m.

Himd[VO_2(2,6-pydc)] (**5**) was prepared according to procedures B and C. Yield: *m* = 111 mg (70%), CHN elemental analysis: calculated for $C_{10}H_8N_3O_6V$ (%): C 37.87, H 2.54, N 13.25; found: C 37.92, H 2.35, N 13.22. IR (ATR, cm^{-1}): 3160br, 3130m, 3075w, 3048w, 1680s, 1599w, 1563m, 1471w, 1424w, 1397w, 1337s, 1176m, 1150w, 1101w, 1069w, 1038w, 1029w, 923s, 907s, 803s, 768m, 745s, 670s, 627s.

Crystallography

Single-crystal X-ray diffraction data were collected at room temperature (**1**, **3**, **4**·H_2O, **5**) or at 150 K (**1**·2H_2O, **2**·H_2O, **3**·H_2O) either on a Nonius Kappa CCD Diffractometer or an Agilent Technologies SuperNova Dual diffractometer with an Atlas detector using monochromated Mo-K_α radiation (λ = 0.71073 Å) (**1**, **3**, **4**·H_2O, **5**) or Cu-K_α radiation (λ = 1.54184 Å) (**1**·2H_2O, **2**·H_2O, **3**·H_2O). The data were processed using DENZO[28] or CrysAlis Pro.[29] The structures were solved by direct methods using the program SHELXS-97[30] (**1**·2H_2O), SIR97[31] (**1**, **2**·H_2O, **3**, **4**·H_2O, **5**) or SIR2004[32] (**3**·H_2O), and refined on F^2 using full-matrix least-squares procedures (SHELXL-97).[30] All non-hydrogen atoms were refined anisotropically, except atoms of a minor part (34%) of disordered 4-aminopyridinium cation in **3**·H_2O. In **4**·H_2O the water molecule (O6) and the hydrogen atoms in the methyl groups of the Hdmap cation are disordered over the mirror plane in 0.50 : 0.50 ratio. Hydrogen atoms on aromatic rings, methyl, amino and hydroxyl groups were treated as riding atoms in geometrically idealized positions. Hydrogen atoms on water molecules were located from difference Fourier maps and refined by fixing the bond lengths and isotropic temperature factors as U_{iso}(H) = 1.5U_{eq}(O). Crystallographic data are summarized in Table 1.

Table 1 Crystal data and structure refinement details for compounds **1–5**

	1·2H$_2$O	**1**	**2**·H$_2$O	**3**·H$_2$O	**3**	**4**·H$_2$O	**5**
Formula	$C_{12}H_{13}N_2O_8V$	$C_{12}H_9N_2O_6V$	$C_{12}H_{11}N_2O_8V$	$C_{12}H_{12}N_3O_7V$	$C_{12}H_{10}N_3O_6V$	$C_{14}H_{16}N_3O_7V$	$C_{10}H_8N_3O_6V$
M_r	364.18	328.15	362.17	361.19	343.17	389.24	317.13
T (K)	150(2)	293(2)	150(2)	150(2)	293(2)	293(2)	293(2)
Crystal system	Triclinic	Triclinic	Monoclinic	Monoclinic	Monoclinic	Orthorhombic	Monoclinic
Space group	$P\bar{1}$	$P\bar{1}$	$P2_1/m$	$P2_1/m$	$P2_1/c$	$Pbcm$	$C2$
a (Å)	6.7436(3)	7.9144(3)	7.8481(2)	8.1855(2)	14.4966(3)	8.17150(10)	9.3492(9)
b (Å)	8.1400(3)	12.5749(7)	6.42100(10)	6.5443(2)	7.3713(2)	29.4539(5)	12.4260(5)
c (Å)	13.7971(5)	13.4045(6)	13.8887(3)	13.8669(3)	14.6252(3)	6.63980(10)	6.4360(7)
α (°)	103.904(4)	88.379(3)	90.00	90.00	90.00	90.00	90.00
β (°)	97.539(3)	89.985(2)	95.055(2)	97.755(2)	118.6960(10)	90.00	129.421(17)
γ (°)	95.474(4)	74.931(3)	90.00	90.00	90.00	90.00	90.00
Volume (Å^3)	722.45(5)	1287.63(10)	697.17(3)	736.03(3)	1370.88(5)	1598.08(4)	577.59(9)
Z	2	4	2	2	4	4	2
D_c (Mg m^{-3})	1.674	1.693	1.725	1.630	1.663	1.618	1.823
μ (mm^{-1})	6.192	0.801	6.416	6.041	0.758	0.665	0.891
F(000)	372	664	368	368	696	800	320
Crystal size (mm)	0.50 × 0.20 × 0.17	0.13 × 0.08 × 0.08	0.40 × 0.20 × 0.05	0.40 × 0.25 × 0.07	0.50 × 0.22 × 0.12	0.25 × 0.18 × 0.03	0.30 × 0.30 × 0.30
Reflections collected	6961	10594	3489	3693	5849	3499	3063
Reflections unique (R_{int})	2950 (0.0299)	5902 (0.0598)	1552 (0.0267)	1627 (0.0267)	3137 (0.0147)	1987 (0.0177)	1484 (0.0193)
Parameters	220	379	140	159	199	160	93
R, wR_2 [$I > 2\sigma(I)$][a]	0.0395, 0.1105	0.0532, 0.1162	0.0333, 0.0913	0.0362, 0.1009	0.0320, 0.0866	0.0323, 0.0825	0.0247, 0.0560
R, wR_2 (all data)[b]	0.0402, 0.1114	0.1365, 0.1504	0.0335, 0.0916	0.0367, 0.1018	0.0412, 0.0933	0.0429, 0.0879	0.0257, 0.0577
GOF, S[c]	1.044, 1.043	0.964	1.089, 1.090	1.058	1.063	1.054	1.087
Extinction coefficient			0.0144(14)	0.023(2)			
Flack parameter							0.019(18)

[a] $R = \sum||F_o| - |F_c||/\sum|F_o|$. [b] $wR_2 = \{\sum[w(F_o^2 - F_c^2)^2]/\sum[w(F_o^2)^2]\}^{1/2}$. [c] $S = \{\sum[(F_o^2 - F_c^2)^2]/(n/p)\}^{1/2}$ where n is the number of reflections and p is the total number of parameters refined.

Results and discussion

Synthesis and spectroscopic properties

Seven structures of dioxido(pyridine-2,6-dicarboxylato)vanadate(v) salts with pyridinium (Hpy$^+$), 2-hydroxypyridinium (H2pyon$^+$), 4-aminopyridinium (H4apy$^+$), 4-(dimethylamino)pyridinium (Hdmap$^+$), and imidazolium (Himd$^+$) counterions were determined. Colourless to pale yellow vanadium(v) pyridine-2,6-dicarboxylic complexes were isolated from aqueous or alcoholic mixtures of the ammonium or sodium metavanadate, pyridine-2,6-dicarboxylic acid (dipicolinic acid) and imidazole or pyridine analogues stirred at 70 °C for 15–30 minutes. After slow evaporation of solvents, crystals of **1**·2H$_2$O, **2**·H$_2$O, **3**·H$_2$O, **4**·H$_2$O and **5** were grown from the solutions. We have also attempted to prepare vanadium(IV) complexes with the pyridine-2,6-dicarboxylato ligand. However, when combining vanadyl sulphate with esters of pyridine-2,6-dicarboxylic acid and the corresponding nitrogen base only vanadium(v) complexes were obtained in rather low yields. In all these cases vanadium(IV) turned into vanadium(v) and the same structures, *i.e.* **2**·H$_2$O and **4**·H$_2$O, **5** were obtained, except in the case of 4apy and py where the anhydrous **1** and **3** were formed. We have observed that monohydrate **3**·H$_2$O and dihydrate **1**·2H$_2$O are unstable outside the solution. When exposed to air, crystals of **3**·H$_2$O decompose, lose the crystal water, and, with the respect to the elemental analysis and IR spectra, transform into anhydrous compound **3**. Crystals of dihydrate **1**·2H$_2$O also decompose, but lose only one equivalent of crystal water, as confirmed by elemental analysis.

The symmetric and asymmetric stretching vibrations of the VO_2^+ moiety are observed in the range 951–907 cm^{-1} and have a shape of shoulder or are split into two or three bands. The position of these bands is similar to those in the NH$_4$[VO$_2$(2,6-pydc)] complex.[33] Strong characteristic bands of the carboxyl groups are observed in the range 1695–1656 cm^{-1} for the asymmetric vibrations (ν_{as}) and 1342–1333 cm^{-1} for the symmetric vibrations (ν_s). The difference between asymmetric and symmetric stretching vibrations ($\Delta = \nu_{as} - \nu_s$) of the carboxylate groups between 319 and 352 cm^{-1} is in accordance with monodentate coordination to the VO_2^+ moiety.[34] The vibrational modes corresponding to aromatic C–H vibrations in all compounds appear in the range 3178–3050 cm^{-1}. For compound **4**·H$_2$O also weak vibrations in the range 2964–2870 cm^{-1} are present, which could correspond to the vibrations of the methyl groups of the Hdmap cation. Compounds **1**·2H$_2$O, **2**·H$_2$O and **4**·H$_2$O show additional broad IR bands in the range 3506–3365 cm^{-1} corresponding to the O–H stretching vibrations of the crystal water.

Description of X-ray crystal structures

Structure of the dioxido(pyridine-2,6-dicarboxylato-*N*,*O*,*O*′)-vanadate(v) anion. All of the compounds contain mononuclear dioxido(pyridine-2,6-dicarboxylato-*N*,*O*,*O*′)vanadate(v) anion. The vanadium atom in [VO$_2$(2,6-pydc)]$^-$ has a distorted square-pyramidal coordination environment, with two oxido oxygen atoms in a mutual *cis* position and a pyridine-2,6-dicarboxylato ligand coordinated to the VO_2^+ moiety in a tridentate manner

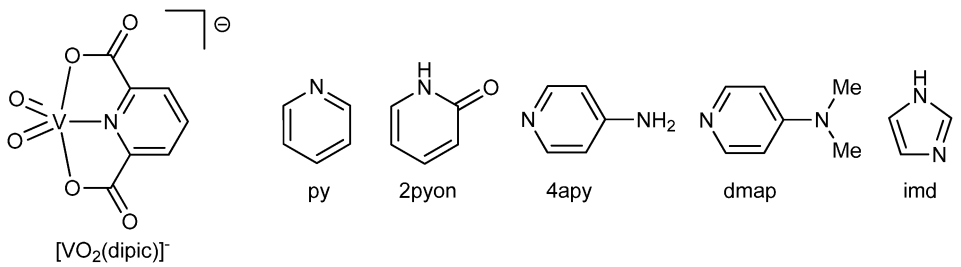

Scheme 1 Structure of the $[VO_2(2,6\text{-pydc})]^-$ anion with tridentate coordination of the pyridine-2,6-dicarboxylate ligand and the nitrogen bases used to form counterions.

through the pyridyl nitrogen atom and two carboxylate oxygen atoms (Scheme 1).

Selected bond distances and angles for individual complexes are summarized in Tables S1 and S2 (in ESI†), respectively. The bond distances between vanadium and pyridyl nitrogen atoms for all complexes are in the range 2.0824(19)–2.0993(13) Å, the distances between vanadium and carboxylate oxygen atoms are slightly shorter and are in the range 1.9746(17)–2.0109(17) Å. Double bonds between vanadium and oxido oxygen atoms of 1.6078(14)–1.6311(14) Å are as expected the shortest bonds in complexes.

Distortion of the pentacoordinated structure due to the chelation of the pyridine-2,6-dicarboxylato ligand is even more evident from the observed bond angles around vanadium. Angles between carboxylate oxygen atoms and pyridyl nitrogen atom are 73.86(5)–75.02(4)°, and angles between carboxylate oxygen atoms are 147.97(5)–150.04(7)°. Angles between carboxylate oxygen atoms and oxido oxygen atoms are 97.92(15)–100.15(15)°, and angles between two oxido oxygen atoms are in the range of 107.92(7)–110.49(13)°. These bond distances and angles are in the same range as previously reported for ammonium, guanidinium[33] and 2,9-dimethyl-1,10-phenanthrolinium[35] compounds. The distortion of a square-pyramid can be best described by the structural parameter τ (0 for an ideal square pyramid and 1 for an ideal trigonal bipyramid),[36] which in these cases is in the range 0.38–0.42, except for **3** and **1**·2H_2O where it is 0.16 and 0.35, respectively. This difference will be discussed later.

The vanadium atom in **2**·H_2O, **3**·H_2O, **4**·H_2O and **5** lies in the plane with the pyridine-2,6-dicarboxylate O and N binding atoms; however, in other compounds vanadium is positioned above this plane for 0.047 Å (**1**·2H_2O), 0.036 and 0.030 Å (**1**), and 0.157 Å (**3**).

Pyridinium dioxido(pyridine-2,6-dicarboxylato-*N*,*O*,*O*′)vanadate(v) (1) and dihydrate (1·2H_2O). Pyridinium salt crystallizes either as a dihydrate (**1**·2H_2O) or as an anhydrous (**1**) form. Compound **1**·2H_2O crystallizes in the triclinic space group $P\bar{1}$. One asymmetric unit of **1**·2H_2O contains one complex anion, one cation and two molecules of crystal water (Fig. S1, ESI†). Hydrogen bonds and weak C–H···O interactions found in **1**·2H_2O are listed in Table S3 (in ESI†). In **1**·2H_2O only the protonated pyridinium group would act as the hydrogen bond donor, but due to the additional water molecules more diverse hydrogen bonding is possible. Water molecules act as hydrogen bond donors and hydrogen bond acceptors, and exhibit linkage between adjacent anions and cations. Infinite chains of anions parallel to vector [110] with the $C^2_2(12)$ graph set[37] motif are formed *via* O–H···O ($d_{D\cdots A}$ = 2.80–2.88 Å) hydrogen bonds between anions and water molecules and *via* O–H···O ($d_{D\cdots A}$ = ∼2.67 Å) hydrogen bonds between two water molecules. These chains are further connected into parallel pairs *via* O–H···O ($d_{D\cdots A}$ = ∼2.81 Å) hydrogen bonds forming flat bands with $R^6_6(24)$ and $R^4_4(16)$ graph set motifs. To the water molecules on the sides of the band pyridinium cations are hydrogen-bonded *via* charge-assisted N–H···O hydrogen bonds ($d_{D\cdots A}$ = ∼2.66 Å) (Fig. 1). Additional stabilization of the crystal lattice is provided by weak C–H···O and π···π stacking interactions. Weak π···π stacking interactions connect pairs of parallel pyridinium rings with a centroid-to-centroid distance of 4.1093(13) Å that belong to the adjacent hydrogen-bonded bands and stabilize packing of hydrogen-bonded bands along [101] (Table S8, ESI†). Packing is facilitated in all three dimensions by C–H···O interactions ($d_{D\cdots A}$ = 3.15–3.27 Å) (Fig. 1).

Anhydrous pyridinium salt **1** also crystallizes in the triclinic space group $P\bar{1}$. One asymmetric unit of anhydrous **1** contains two complex anions and two cations (Fig. S2, ESI†). Hydrogen bonds and weak C–H···O interactions found in anhydrous **1** are listed in Table S3 (in ESI†). Due to the absence of crystal water, only two hydrogen bonds could be formed in one asymmetric unit of the anhydrous compound **1**. Furthermore, both cations in the asymmetric unit are connected to the same anion *via* N–H···O hydrogen bonds with the $D^1_1(2)$ graph set motifs. The first pyridinium cation is hydrogen-bonded to carboxylate O7 atom ($d_{D\cdots A}$ = ∼3.13 Å), and the second cation is hydrogen-bonded to the oxido O11 atom ($d_{D\cdots A}$ = ∼2.88 Å). The second vanadium anion is not involved in the hydrogen bonding (Fig. 2).

Interestingly, due to the lack of strong non-covalent intermolecular interactions such as hydrogen bonds anions are involved to a larger extent in weak interactions. For instance, weak V=O···C interactions previously described by Stilinović *et al.*[25] have been observed between the adjacent V1 and V2 complex anions of the asymmetric unit. The V=O···C interactions are formed between oxido groups and carboxyl carbon atoms with O···C distances of 2.968(5) and 3.039(5) Å and V=O···C angles of 139.1(2) and 141.0(2)°. Ions of different asymmetric units are further connected only by weak C–H···O and π···π stacking interactions. π···π stacking interactions were observed along the *a* axis between pairs of cations that

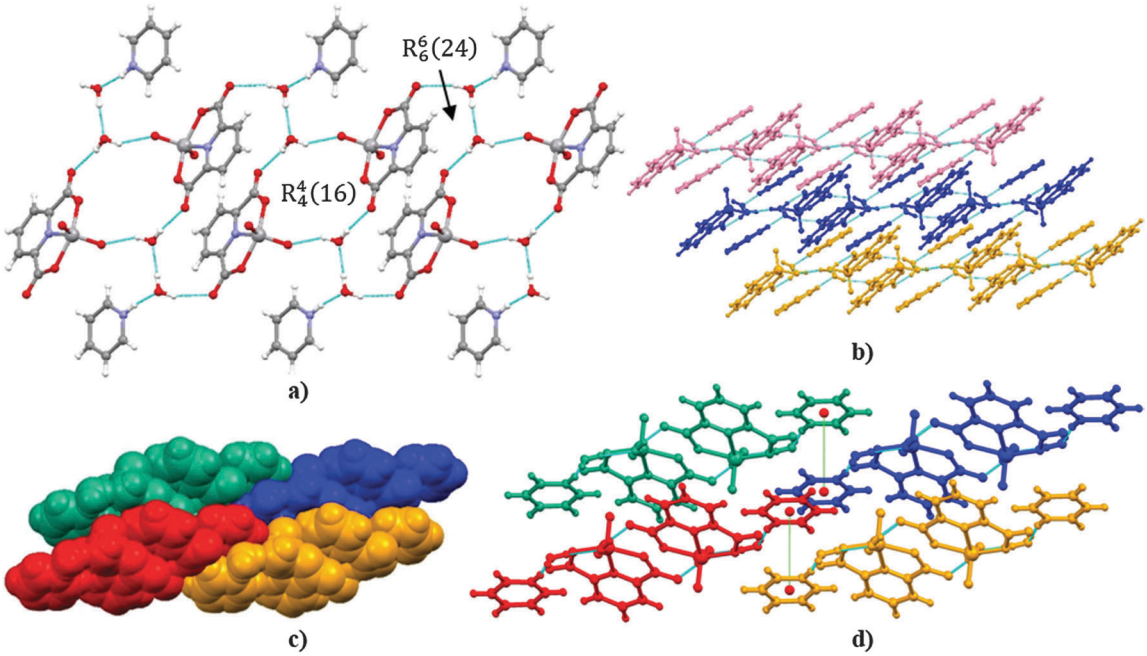

Fig. 1 Hydrogen bonding network in **1**·2H_2O. (a) A fragment of hydrogen-bonded band with $R^6_6(24)$ and $R^4_4(16)$ graph set motifs. (b) Packing of adjacent bands by C–H···O interactions. (c) Space filled representation of the three-dimensional packing along the [110] direction. (d) Packing diagram with π···π stacking interactions between cation rings.

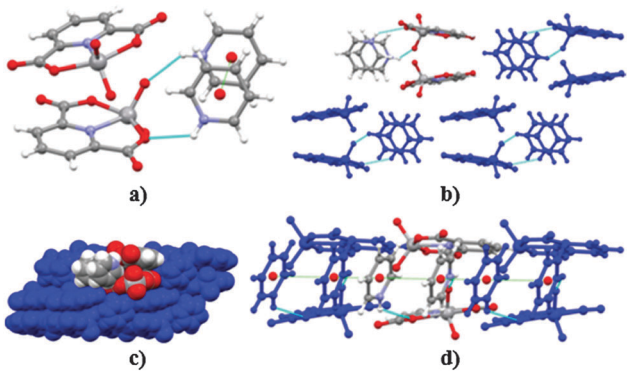

Fig. 2 Hydrogen bonding network in anhydrous **1**. (a) Hydrogen bonds and π···π stacking interaction in the asymmetric unit of anhydrous **1**. (b) Packing diagram along the *a* axis facilitated by weak interactions. (c) Space filled representation of packing along the [110] direction. (d) Packing diagram emphasizing the π···π stacking interactions.

belong to the same asymmetric unit with a centroid-to-centroid distance of 3.878(4) Å and an inter-ring dihedral angle of 6.3(3)°, and between cations of the adjacent asymmetric units with a centroid-to-centroid distance of 4.230(4) Å (Fig. 2, Table S8, ESI†). Supramolecular architecture is therefore controlled by additional weak hydrogen bonds extending in all three dimensions between aromatic CH groups of Hpy^+ and V2 anions, oxido and carbonyl oxygen atoms of V1 anions, and oxido and carboxyl oxygen atoms of V2 anions (Fig. 2).

2-Hydroxypyridinium dioxido(pyridine-2,6-dicarboxylato-*N*,*O*,*O*′)-vanadate(v) monohydrate (2·H_2O). 2-Hydroxypyridinium salt 2·H_2O crystallizes in the monoclinic space group $P2_1/m$. One asymmetric unit of 2·H_2O contains one half of the complex anion, one half of the cation and one half of the water molecule, which lie on the mirror plane parallel to the *ac* plane (Fig. S3, ESI†). Hydrogen bonds and weak C–H···O interactions found in 2·H_2O are listed in Table S4 (in ESI†). The ionic pair on the symmetry plane is connected *via* an O–H···O hydrogen bond ($d_{D\cdots A}$ = ~2.58 Å) involving the hydroxyl moiety of $H2pyon^+$ and the carbonyl oxygen atom of the 2,6-$pydc^{2-}$ ligand. An infinite square pillar is formed along the *b* axis due to the connection of ionic pairs through water molecules forming an $R^6_6(24)$ motif *via* charge-assisted N–H···O ($d_{D\cdots A}$ = ~2.67 Å) and O–H···O ($d_{D\cdots A}$ = ~2.81 Å) hydrogen bonding connecting NH moieties of H2pyon through water molecules to oxido atoms of the VO_2^+ moiety. Hence, the pillar structure is a consequence of strong hydrogen bonding interactions between the polar hydrophilic regions and leads to the exposure of the hydrophobic region to the exterior. Such organization and separation of hydrophobic and hydrophilic regions has an important influence on supramolecular arrangement.[38]

The three-dimensional framework is achieved by connecting the pillars to each other by several C–H···O interactions ($d_{D\cdots A}$ = 3.14–3.48 Å) (Fig. 3). However, no significant π···π interactions have been observed. View of the packing along the *b*-axis reveals formation of canals between anions and cations that are parallel to the *b*-axis and are occupied by water molecules (Fig. 4).

4-Aminopyridinium dioxido(pyridine-2,6-dicarboxylato-*N*,*O*,*O*′)-vanadate(v) (3) and monohydrate (3·H_2O). 4-Aminopyridinium salt crystallizes as a monohydrate 3·H_2O or in its anhydrous form **3**. 3·H_2O crystallizes in the monoclinic space group $P2_1/m$. Cation, complex anion and a water molecule lie on a mirror plane. One asymmetric unit of 3·H_2O therefore contains one half of each

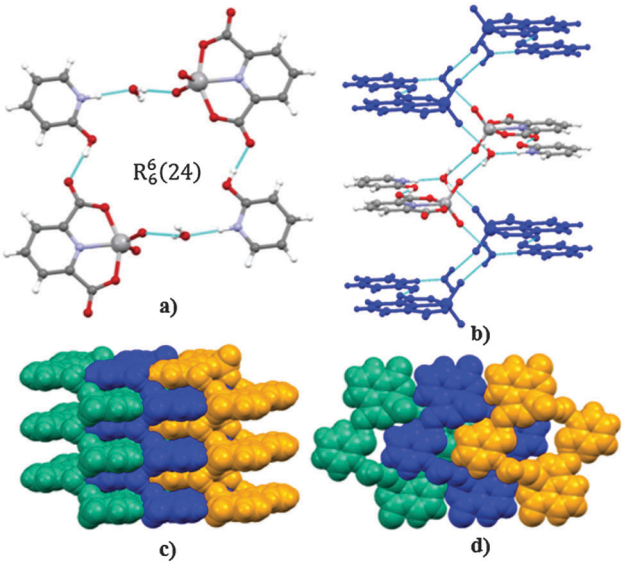

Fig. 3 Hydrogen bonding network in **2**·H_2O. (a) A fragment of the crystal structure of **2**·H_2O emphasizing the connection of ionic pairs through a water molecule *via* the $R^6_6(24)$ graph set motif. (b) Square pillar formation due to the hydrogen bonding. (c) Space filled representation of the packing. (d) Space filled representation of the packing along the *b*-axis.

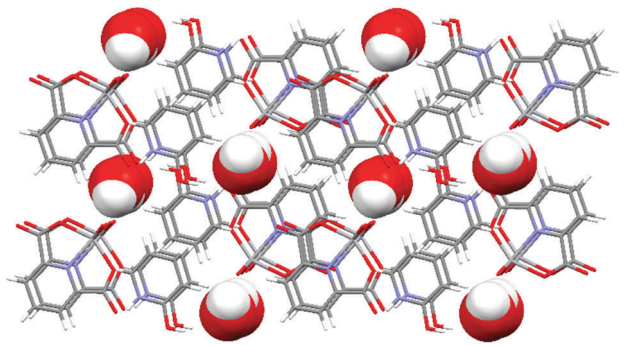

Fig. 4 Packing of **2**·H_2O along the *b*-axis showing the canals filled with water molecules. Water molecules are shown as space-filling models for clarity.

anion, cation and a half of the water molecule (Fig. S4, ESI†). The 4-aminopyridinium cation is disordered over two coplanar positions with a ratio of 0.66 : 0.34. The centers of both rings lie almost at the same position, but the cations are rotated for approximately 135°. Both possible cation positions enable similar hydrogen bonding as shown in Fig. 5. Hydrogen bonds found in **3**·H_2O are listed in Table S5 (in ESI†).

The Coulomb interactions between H4apy$^+$ cations and $[VO_2(2,6\text{-pydc})]^-$ anions supported by charge-assisted hydrogen bonding between them organize chain formation. Cations and anions on the symmetry plane are connected *via* N–H···O hydrogen bonds ($d_{D\cdots A}$ = 2.77–2.84 Å for the main component) along the *c* axis with the $C^2_2(12)$ graph set motif involving NH and NH_2 moieties of H4apy (donors) and the carboxyl and carbonyl oxygen atoms of the 2,6-pydc^{2-} ligand (acceptors). This chain is further connected to adjacent chains through water molecules forming an $R^6_6(26)$ motif *via* O–H···O ($d_{D\cdots A}$ = ~2.76 Å) and N–H···O ($d_{D\cdots A}$ = ~2.82 Å for the main component) hydrogen bonds connecting the NH_2 moiety through a water molecule to the oxido oxygen atom of the VO_2^+ moiety (Fig. 6). Such two-dimensional frameworks are packed into crystal structure; however, no significant C–H···O or π···π interactions have been observed among them. View of the packing along the *b*-axis reveals a similar structure to that in **2**·H_2O. Between anions and cations canals parallel to the *b*-axis filled with water are formed (Fig. 7).

Anhydrous 4-aminopyridinium salt **3** crystallizes in the monoclinic space group $P2_1/c$. One asymmetric unit of anhydrous **3** contains one complex anion and one H4apy$^+$ cation (Fig. S5, ESI†). Similar to the **3**·H_2O structure the amino group and the protonated pyridine group in H4apy$^+$ act as hydrogen bond donors, but only one oxido and two carboxyl oxygen atoms act as hydrogen bond acceptors. Hydrogen bonds found in anhydrous **3** are listed in Table S5 (ESI†).

As mentioned earlier the structural parameter τ describing the distortion of a square-pyramid is noticeably smaller for anhydrous **3** (τ = 0.16) than for all the other complex anions (τ = 0.35–0.42). The parameter τ is based on the difference between the largest two X–M–X angles α and β in the complex according to the equation $\tau = (\alpha - \beta)/60°$.[33] We have investigated the reasons for such unexpected difference in τ values in the same type of complexes and observed that the largest angle α is $O_{carboxyl}$–V–$O_{carboxyl}$, and has similar values in all compounds (~148°); however, the second largest angle β is N–V–O_{oxido} and is close to 125° in all cases, except in the anhydrous **3** being 138.42(7)°. This larger angle β (N1–V1–O6) in anhydrous **3** causes a small tilt of a VO_2^+ group, as can be observed also by a smaller N1–V1–O5 angle (113.63(7)°). The distortion of the VO_2^+ moiety probably happens due to the involvement of only one oxido oxygen atom of the VO_2^+ moiety in the hydrogen bonding. This has also an effect on the difference in V=O bond lengths of the VO_2^+ moiety (1.6311(14) *vs.* 1.6078(14) Å), which is the largest difference in all compounds.

Coulomb interactions between H4apy$^+$ cations and $[VO_2(2,6\text{-pydc})]^-$ anions supported by charge-assisted hydrogen bonding between them organize the packing of cations and anions. Cations and anions are connected *via* N–H···O hydrogen bonds ($d_{D\cdots A}$ = 2.78–3.00 Å) into infinite chains with the $C^6_6(30)$ graph set motif involving NH and NH_2 moieties of H4apy and one oxido oxygen of the VO_2^+ moiety as well as the carboxyl and carbonyl oxygen atoms of the 2,6-pydc^{2-} ligand. Chains are further connected into infinite double layers perpendicular to the *c* axis by $R^4_4(16)$ and $R^8_8(44)$ graph set motifs. Further stabilization of the crystal lattice is enabled by weak C–H···O interactions between cations and anions ($d_{D\cdots A}$ = 3.08–3.23 Å) or between adjacent anions ($d_{D\cdots A}$ = ~3.48 Å) that help to connect two-dimensional layers into a three-dimensional framework (Fig. 8). No significant π···π stacking has been observed in this crystal structure.

4-(Dimethylamino)pyridinium dioxido(pyridine-2,6-dicarboxylato-*N*,*O*,*O*′)vanadate(v) monohydrate (4·H_2O). 4-Dimethylaminopyridinium salt **4**·H_2O crystallizes in the orthorhombic

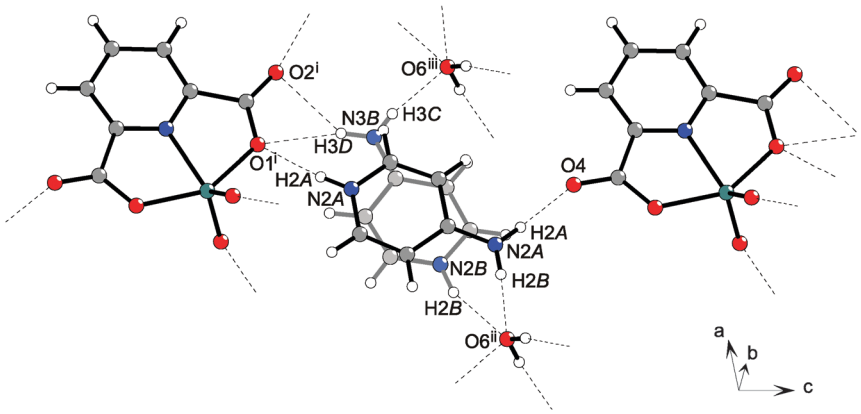

Fig. 5 The possibility of the formation of hydrogen bonds for both positions of a disordered 4-aminopyridinium cation in **3**·H_2O. Dashed lines indicate hydrogen bonds (symmetry codes: (i) *x*, *y*, *z* − 1; (ii) −*x*, *y* + 1/2, −*z* + 1; (iii) −*x* + 1, *y* + 1/2, −*z* + 1).

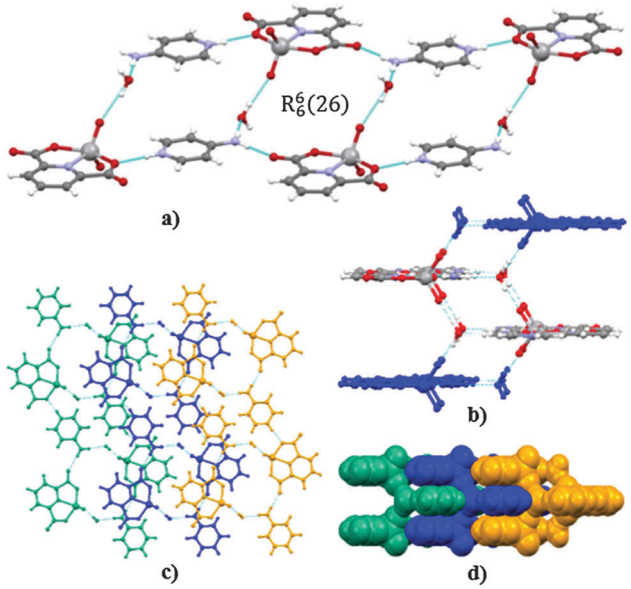

Fig. 6 Hydrogen bonding network in **3**·H_2O for the major part of a disordered 4-aminopyridinium cation. (a) A fragment of the crystal structure of **3**·H_2O emphasizing the connection of adjacent chains through a water molecule *via* the $R^6_6(26)$ graph set motif. (b) Chains connected into a two-dimensional framework. (c) Packing diagram along the *b*-axis. (d) Space filled representation of the packing along the *c*-axis.

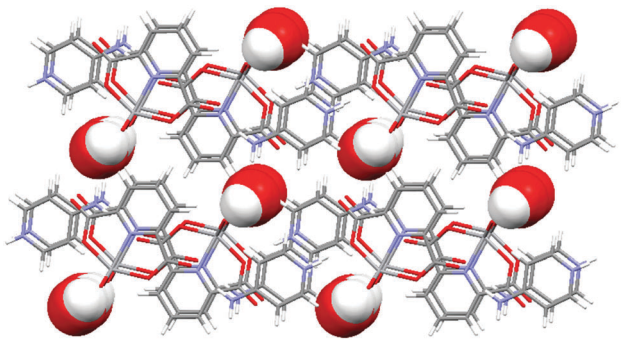

Fig. 7 Packing of **3**·H_2O along the *b*-axis showing the canals filled with water molecules. Water molecules are shown as space-filling models for clarity.

space group *Pbcm*. One asymmetric unit of **4**·H_2O contains one half of the anion and cation and a half of the water molecule (Fig. S6, ESI†) due to a mirror plane parallel to the *ab* plane. Water molecule and methyl protons of the cation are disordered over two symmetry related positions with a ratio of 0.50 : 0.50 due to the mirror plane. Hydrogen bonds found in **4**·H_2O are listed in Table S6 (in ESI†). In **4**·H_2O, beside a water molecule, only a protonated pyridine group of the $Hdmap^+$ cation acts as a hydrogen bond donor, while the two oxido and two carboxyl oxygen atoms of the anion act as hydrogen bond acceptors. Adjacent anions are connected through water molecules *via* O–H···O hydrogen bonds ($d_{D\cdots A}$ = 3.07–3.14 Å) into twisted infinite chains. Chains are parallel to the *c* axis and (with the omission of one part of the disordered water molecule) possess the $C^4_4(6)$ graph set motif involving water molecules as donors, and carbonyl and oxido oxygen atoms as acceptors. To the water molecules belonging to these chains also cations are connected *via* charge-assisted N–H···O hydrogen bonds ($d_{D\cdots A}$ = ∼2.82 Å). Stabilization of the crystal structure is further controlled by weak hydrogen bonds, as well as π···π stacking interactions listed in Table S8 (ESI†). The π···π stacking spreading along the *c* axis has been observed between parallel 2,6-$pydc^{2-}$ and $Hdmap^+$ rings with a centroid-to-centroid distance of 3.87 Å that are part of two different hydrogen-bonded chains, and helps to stabilize packing along the *a* axis. Weak C–H···O interactions ($d_{D\cdots A}$ = 3.22–3.46 Å) formed between methyl and aromatic hydrogen atoms of cations and oxygen atoms of anions spread along *a* and *b* axes, and stabilize packing of **4**·H_2O in all three dimensions (Fig. 9). View of the packing diagram along the *c*-axis reveals formation of canals between anions and cations parallel to the *c*-axis. Canals are wider than in **2**·H_2O and **3**·H_2O, and contain two rows of water molecules (Fig. 10).

Imidazolium dioxido(pyridine-2,6-dicarboxylato-*N*,*O*,*O*′)-vanadate(v) (5). Imidazolium salt **5** crystallizes in the orthorhombic space group *C*2. One asymmetric unit of **5** contains one half of the anion and a half of the cation (Fig. S7, ESI†) that lie on a two-fold screw axis parallel to *b*. Hydrogen bonds and weak C–H···O interactions found in **5** are listed in Table S7 (in ESI†). Cations and anions in **5** are connected *via* N–H···O

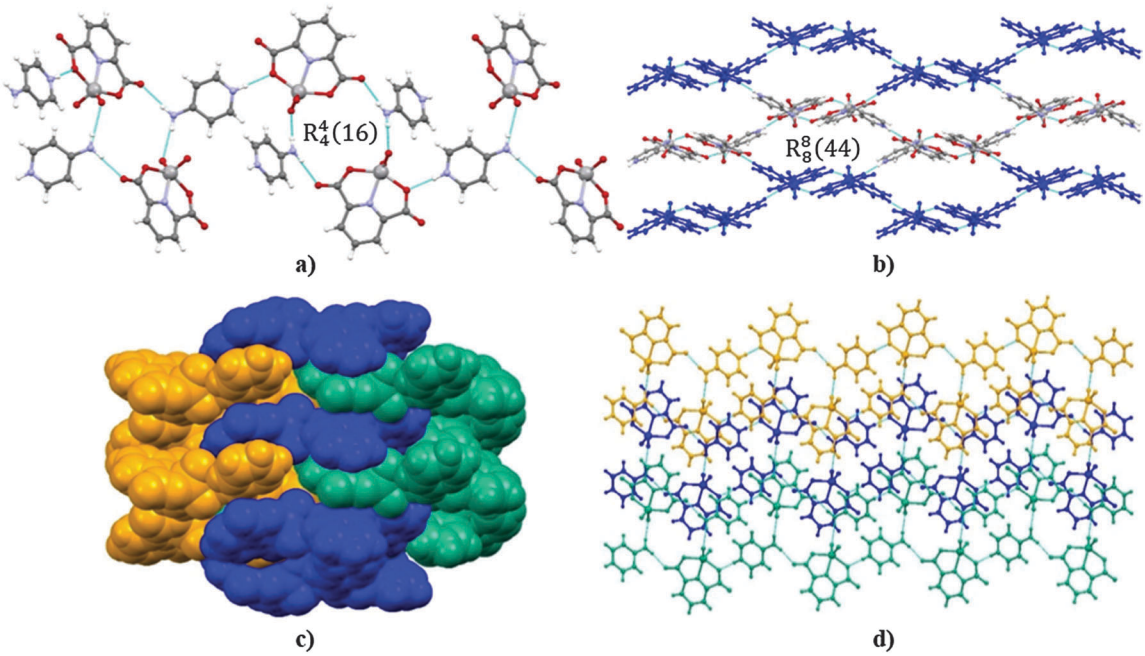

Fig. 8 Hydrogen bonding network in anhydrous **3**. (a) A fragment of the crystal structure of **3** emphasizing the connection of cations and anions *via* the $R^4_4(16)$ graph set motif. (b) View along the *c* axis on the two-dimensional framework emphasizing the $R^8_8(44)$ motif. (c) Space filled representation of the packing of layers facilitated by weak C–H···O interactions. (d) Packing diagram along the *b* axis.

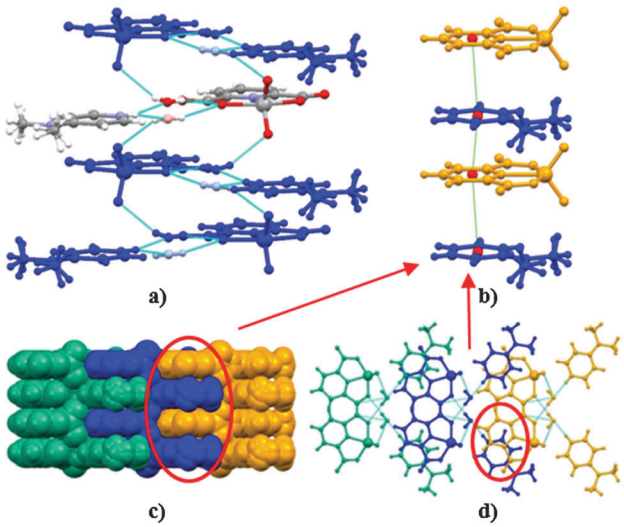

Fig. 9 Hydrogen bonding network in **4**·H_2O. (a) A hydrogen-bonded chain parallel to the *c* axis with the $C^4_4(12)$ motif. (b) π···π stacking interactions between parallel anions and cations. (c) Space filled representation and packing diagram along the *b* axis indicating π···π stacking interactions. (d) Packing diagram along the *c* axis (facilitated by weak interactions).

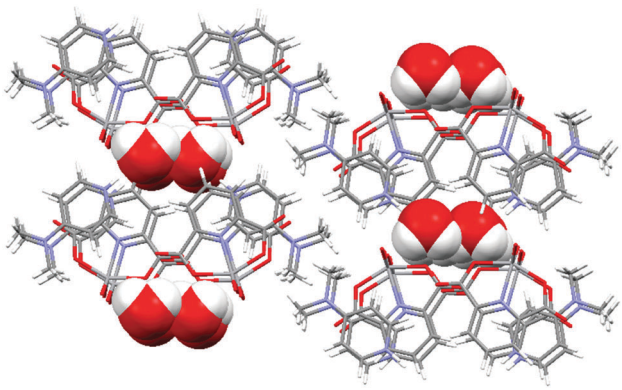

Fig. 10 Packing of **4**·H_2O along the *c*-axis showing the canals filled with water molecules. Water molecules are shown as space-filling models for clarity.

hydrogen bonds ($d_{D\cdots A}$ = ~2.83 Å) along [10−1] with the $C^2_2(12)$ graph set motif involving NH moieties of the imidazolium cation and carboxyl oxygen atoms of the 2,6-pydc^{2-} ligand. This chain is further connected with adjacent chains into a three-dimension framework with the $R^6_5(24)$ and $R^6_5(28)$ graph set motifs *via* additional N–H···O hydrogen bonds ($d_{D\cdots A}$ = ~2.80 Å) involving oxido oxygen atoms of the VO_2^+ moiety as well (Fig. 11). Thus, the three-dimensional structure is organized through the Coulomb interactions between imidazolium cations and $[VO_2(2,6\text{-pydc})]^-$ anions supported by bifurcated charge-assisted hydrogen bonding between protonated imidazolium NH groups as hydrogen bond donors, while oxido and carboxyl oxygen atoms of the anions act as hydrogen bond acceptors. The crystal lattice of **5** is additionally stabilized by weak C–H···O and π···π stacking interactions. The π···π stacking interactions extending along the [101] direction are formed between almost parallel $Himd^+$ and 2,6-pydc^{2-} aromatic rings (Table S8) with a dihedral angle of 0.34(10)° and a centroid-to-centroid distance of 3.6787(13) Å (Fig. 11). Weak C–H···O interactions spreading in all three dimensions are formed between carboxyl oxygen and aromatic hydrogen atoms of the

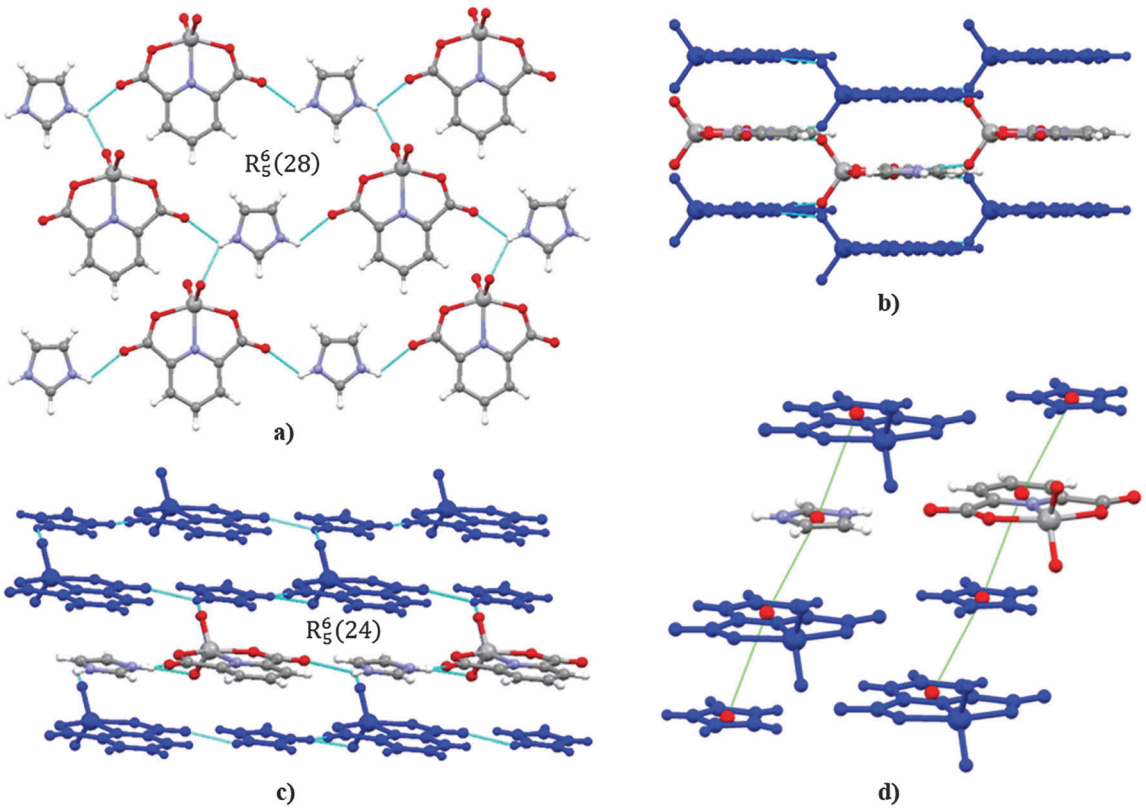

Fig. 11 Hydrogen bonding network in **5**. (a) A fragment of the hydrogen bonding in **5** with the $R^6_5(28)$ graph set motif. (b) Packing along the [1,0,−1] direction. (c) Packing diagram with the $R^6_5(24)$ graph set motif. (d) π···π stacking interactions between anions and cations.

2,6-pydc^{2-} ligand ($d_{D\cdots A}$ = ∼3.36 Å) or along the *c* axis between imidazolium CH groups and carboxylate oxygen atoms of the anions ($d_{D\cdots A}$ = ∼3.32 Å).

Structural comparison

The vanadium center in the dioxido(pyridine-2,6-dicarboxylato)-vanadate(v) anion has a distorted square-pyramidal structure. Distortion also depends on the presence of hydrogen bonding. In most cases both oxido oxygen atoms are involved in the hydrogen bonding and both V=O bond lengths are of the same range. The value of trigonality parameter τ in these compounds is usually 0.38–0.42. However, in **1**·2H$_2$O and **3** only one oxido oxygen atom is involved in the hydrogen bonding and this V=O distance is elongated compared to the others. Interestingly, in these two compounds the distortion of the vanadium coordination sphere is the least pronounced, as can be seen by the τ values (in **1**·2H$_2$O is 0.35 and in **3** is 0.16).

In the imidazolium salt, in which each of the two NH groups binds to two acceptors, three-dimensional hydrogen bonding is possible. In 4-aminopyridinium salts with NH and NH$_2$ donating groups two-dimensional systems were observed due to the classical hydrogen bonding. On the other hand, in pyridinium salts with only one donating NH group only isolated or one-dimensional hydrogen bonded systems could be formed and additional packing is stabilized by weak C–H···O and π···π interactions. We have also noticed that the water molecules in the crystal lattice acting as hydrogen bond donors and acceptors additionally increase the number and diversity of hydrogen bonds, but do not necessarily increase the stability of the structures. Powder X-ray diffraction (PXRD) experiments were carried out in order to confirm the phase purity of the bulk materials. We have observed that **1**·2H$_2$O is unstable outside the solution. When exposed to air, crystals of **1**·2H$_2$O decompose and lose one equivalent of crystal water, as confirmed by elemental analysis. Due to this partial dehydration the experimental PXRD pattern of monohydrate **1**·H$_2$O does not correspond with the one computer-simulated from the single crystal data of dihydrate **1**·2H$_2$O (Fig. S8 in ESI†). We have also observed that **3**·H$_2$O is not stable outside the solution. When exposed to air, crystals of **3**·H$_2$O decompose, lose the crystal water, and, with respect to the elemental analysis and IR spectra, transform into anhydrous **3** compound. The experimental PXRD patterns of **2**·H$_2$O, **3**, **4**·H$_2$O and **5** correspond well with the ones computer-simulated from the single crystal data, indicating the high purity of the synthesized samples (Fig. S9 in ESI†). The differences in reflection intensities between the simulated and the experimental pattern are due to the variation in the preferred orientation of the powder samples as well as due to the fact that crystal **2**·H$_2$O was measured at 150 K while all PXRD data were collected at room temperature.

It has to be stressed that vanadium possesses a unique coordination environment in comparison to the other first row transition metals. In addition to the carboxylic group of the 2,6-pydc^{2-} ligand, the [VO$_2$(2,6-pydc)]$^-$ moiety has two

easily accessible oxido oxygen atoms of the VO_2^+ unit. The availability of H-bond donating sites is also reflected in the number of participating acceptors in the $[VO_2(2,6\text{-pydc})]^-$ coordination anion. In **5** with a three-dimensional hydrogen-bonded framework and in **3**·H_2O with a two-dimensional hydrogen-bonded framework four out of six oxygen atoms of the $[VO_2(2,6\text{-pydc})]^-$ anion participate as N/O–H···O hydrogen bond acceptors including both oxido oxygen atoms of the VO_2^+ unit. The number of the acceptor sites of $[VO_2(2,6\text{-pydc})]^-$ anions is reduced to three out of six in **1**·2H_2O, **2**·H_2O and **4**·H_2O with a one-dimensional (band, pillar or chain) hydrogen bonding network and in anhydrous **3** with a two-dimensional hydrogen-bonded framework. However, in **2**·H_2O and **4**·H_2O both oxido oxygen atoms of the VO_2^+ unit participate as acceptors of classical hydrogen bonds while in **1**·2H_2O and **3** only one oxido oxygen atom acts as the acceptor.

Conclusion

We have prepared and structurally characterized seven different dioxido(pyridine-2,6-dicarboxylato)vanadate(v) compounds with aromatic nitrogen cations: pyridinium (**1**·2H_2O and **1**), 2-hydroxypyridinium (**2**·H_2O), 4-aminopyridinium (**3**·H_2O and **3**), 4-(dimethylamino)pyridinium (**4**·H_2O) and imidazolium cation (**5**). The compounds were synthesized *via* different pathways starting either from pyridine-2,6-dicarboxylic acid or its esters. Pyridinium and 4-aminopyridinium salts crystallized depending on the type of preparation either in their hydrous or anhydrous form, while 2-hydroxypyridinium, 4-(dimethylamino)pyridinium and imidazolium salts crystallized in the same way regardless of the synthetic route. The interactions between hydrogen-bonded organic cations and the $[VO_2(2,6\text{-pydc})]^-$ anion has been examined for the formation of self-assembly systems. The unique vanadium coordination environment with two easily accessible oxido oxygen atoms of the VO_2^+ unit is suitable for the construction of non-covalent metal–organic hybrids. In **2**·H_2O, **3**·H_2O, **4**·H_2O and **5** both oxido oxygen atoms of the VO_2^+ unit participate as acceptors, however, in **1**·2H_2O and **3** only one oxido oxygen atom is involved in classical hydrogen bonding. The ability of hydrogen bond formation and especially the number of H-bond donating sites on the cation has a significant impact on the supramolecular structure. In the case of **1**·2H_2O and **4**·H_2O with one H-bond donating Hpy^+ and $Hdmap^+$ cations one-dimensional (band or chain) hydrogen bonding networks *via* N/O–H···O bonds are formed. In **2**·H_2O with two H-bond donating $H2pyon^+$ cation a hydrogen-bonded pillar structure with a hydrophilic interior is formed. On the other hand in the case of the $Himd^+$ cation also with two H-bond donating sites a three-dimensional hydrogen bonding network was observed in **5**. In anhydrous **3** and **3**·H_2O a two-dimensional hydrogen-bonded framework is formed even though the $H4apy^+$ cation possesses the highest number of H-bond donating sites. Besides N/O–H···O hydrogen bonding, also other weak non-covalent interactions, such as C–H···O, π···π, C–H···π and V=O···C interactions play an important role in stabilizing the crystal lattices. Thus, the rational choice of the cation may be an effective way to construct novel metal–organic hybrids with desired structures and properties. This research can be of great help in the field of emerging vanadium hybrid materials particularly from the viewpoint of being aware of the existing building blocks and their binding potentials according to the concepts of crystal engineering.

Acknowledgements

The authors thank the Ministry of Education, Science and Sport of the Republic of Slovenia and the Slovenian Research Agency for financial support (P1–0230–0175) as well as the EN–FIST Centre of Excellence, Trg Osvobodilne fronte 13, 1000 Ljubljana, Slovenia for use of the Supernova diffractometer.

References

1 (*a*) C. B. Aakeröy, N. R. Champness and C. Janiak, *CrystEngComm*, 2010, **12**, 22–43; (*b*) M. G. Goesten, F. Kapteijn and J. Gascon, *CrystEngComm*, 2013, **15**, 9249–9257; (*c*) M. D. Ward and P. R. Raithby, *Chem. Soc. Rev.*, 2013, **42**, 1619–1636; (*d*) M. W. Hosseini, *Coord. Chem. Rev.*, 2003, **240**, 157–166; (*e*) M. M. Safont-Sempere, G. Fernández and F. Würthner, *Chem. Rev.*, 2011, **111**, 5784–5814; (*f*) K. Biradha, C.-Y. Su and J. J. Vittal, *Cryst. Growth Des.*, 2011, **11**, 875–886; (*g*) E. R. Parnham and R. E. Morris, *Acc. Chem. Res.*, 2007, **40**, 1005–1013; (*h*) G. Férey, *Chem. Soc. Rev.*, 2007, **37**, 191–214.

2 (*a*) J. Liu, L. Chen, H. Cui, J. Zhang, L. Zhang and C.-Y. Su, *Chem. Soc. Rev.*, 2014, **43**, 6011–6061; (*b*) A. Dhakshinamoorthy and H. Garcia, *Chem. Soc. Rev.*, 2014, **43**, 5750–5765; (*c*) J. Lee, O. K. Farha, J. Roberts, K. A. Scheidt, S. T. Nguyen and J. T. Hupp, *Chem. Soc. Rev.*, 2009, **38**, 1450–1459.

3 (*a*) B. V. de Voorde, B. Bueken, J. Denayer and D. D. Vos, *Chem. Soc. Rev.*, 2014, **43**, 5766–5788; (*b*) E. Barea, C. Montoro and J. A. R. Navarro, *Chem. Soc. Rev.*, 2014, **43**, 5419–5430; (*c*) J.-R. Li, J. Sculley and H.-C. Zhou, *Chem. Rev.*, 2012, **112**, 869–932.

4 (*a*) Y. He, W. Zhou, G. Qian and B. Chen, *Chem. Soc. Rev.*, 2014, **43**, 5657–5678; (*b*) M. P. Suh, H. J. Park, T. K. Prasad and D.-W. Lim, *Chem. Rev.*, 2012, **112**, 782–835; (*c*) K. Sumida, D. L. Rogow, J. A. Mason, T. M. McDonald, E. D. Bloch, Z. R. Herm, T.-H. Bae and J. R. Long, *Chem. Rev.*, 2012, **112**, 724–781.

5 (*a*) Z. Hu, B. J. Deibert and J. Li, *Chem. Soc. Rev.*, 2014, **43**, 5815–5840; (*b*) Y. Cui, Y. Yue, G. Qian and B. Chen, *Chem. Rev.*, 2012, **112**, 1126–1162; (*c*) L. E. Kreno, K. Leong, O. K. Farha, M. Allendorf, R. P. Van Duyne and J. T. Hupp, *Chem. Rev.*, 2012, **112**, 1105–1125.

6 (*a*) W. Zhang and R.-G. Xiong, *Chem. Rev.*, 2012, **112**, 1163–1195; (*b*) M. Kurmoo, *Chem. Soc. Rev.*, 2009, **38**, 1353–1379.

7 (*a*) L. Brammer, *Dalton Trans.*, 2003, 3145–3157; (*b*) M. Nishio, Y. Umezawa, K. Honda, S. Tsuboyama and H. Suezawa, *CrystEngComm*, 2009, **11**, 1757–1788.

8 (*a*) C. Janiak, *J. Chem. Soc., Dalton Trans.*, 2000, 3885–3896; (*b*) S. M. Malathy Sony and M. N. Ponnuswamy, *Cryst. Growth Des.*, 2006, **6**, 736–742.

9 (*a*) K. Rissanen, *CrystEngComm*, 2008, **10**, 1107–1113; (*b*) L. Brammer, G. M. Espallargas and S. Libri, *CrystEngComm*, 2008, **10**, 1712–1727; (*c*) R. W. Troff, T. Mäkelä, F. Topić, A. Valkonen, K. Raatikainen and K. Rissanen, *Eur. J. Org. Chem.*, 2013, 1617–1637; (*d*) V. G. Saraswatula and B. K. Saha, *New J. Chem.*, 2014, **38**, 897–901.

10 (*a*) S. Petrosyants, Z. Dobrokhotova, A. Ilyukhin and V. Novotortsev, *New J. Chem.*, 2014, **38**, 3803–3812; (*b*) H. S. Jena, *New J. Chem.*, 2014, **38**, 2486–2499; (*c*) M. T. Johnson, Z. Džolić, M. Cetina, O. F. Wendt, L. Öhrström and K. Rissanen, *Cryst. Growth Des.*, 2012, **12**, 362–368; (*d*) F. Perdih, *Monatsh. Chem.*, 2012, **143**, 1011–1017; (*e*) F. Perdih, *J. Coord. Chem.*, 2012, **65**, 1580–1591; (*f*) F. Perdih, *Acta Crystallogr., Sect. C: Cryst. Struct. Commun.*, 2012, **68**, M64–M68; (*g*) F. Perdih, *Struct. Chem.*, 2014, **25**, 809–819.

11 (*a*) H. W. Roesky and M. Andruh, *Coord. Chem. Rev.*, 2003, **236**, 91–119; (*b*) L. Brammer, *Chem. Soc. Rev.*, 2004, **33**, 476–489.

12 I. Cvrtila, V. Stilinović and B. Kaitner, *CrystEngComm*, 2013, **15**, 6585–6593.

13 (*a*) S. S. Sunkari, B. Kharediya, S. Saha, B. Elrezcd and J.-P. Sutter, *New J. Chem.*, 2014, **38**, 3529–3539; (*b*) J. Chen, S.-H. Wang, Z.-F. Liu, M.-F. Wu, Y. Xiao, F.-K. Zheng, G.-C. Guo and J.-S. Huang, *New J. Chem.*, 2014, **38**, 269–276; (*c*) X.-M. Lin, H.-C. Fang, Z.-Y. Zhou, L. Chen, J.-W. Zhao, S.-Z. Zhu and Y.-P. Cai, *CrystEngComm*, 2009, **11**, 847–854; (*d*) S. Macksasitorn, Y. Hu and J. R. Stork, *CrystEngComm*, 2013, **15**, 1698–1705; (*e*) F. Jin, H.-Z. Wang, Y. Zhang, Y. Wang, J. Zhang, L. Kong, F.-Y. Hao, J.-X. Yang, J.-Y. Wu, Y.-P. Tian and H.-P. Zhou, *CrystEngComm*, 2013, **15**, 3687–3695; (*f*) C.-Q. Wan, A.-M. Li, S. A. Al-Thabaiti and T. C. W. Mak, *Cryst. Growth Des.*, 2013, **13**, 1926–1936.

14 (*a*) Y. Wen, T. Sheng, S. Hu, Y. Wang, C. Tan, X. Ma, Z. Xue, Y. Wang and X. Wu, *CrystEngComm*, 2013, **15**, 2714–2721; (*b*) Z. Chen, L. Zhang, F. Liu, R. Wang and D. Sun, *CrystEngComm*, 2013, **15**, 8877–8880; (*c*) R. K. Prajapati, J. Kumar and S. Verma, *CrystEngComm*, 2013, **15**, 9316–9319; (*d*) A. M. Owczarzak, N. Kourkoumelis, S. K. Hadjikakou and M. Kubicki, *CrystEngComm*, 2013, **15**, 3607–3614; (*e*) M. Mirzaei, H. Eshtiagh-Hosseini, M. M. Abadeh, M. Chahkandi, A. Frontera and A. Hassanpoor, *CrystEngComm*, 2013, **15**, 1404–1413; (*f*) V. J. Argyle, L. M. Woods, M. Roxburgh and L. R. Hanton, *CrystEngComm*, 2012, **15**, 120–134; (*g*) A. Singh, R. P. Sharma, T. Aree and P. Venugopalan, *CrystEngComm*, 2013, **15**, 1153–1163.

15 (*a*) P. Thuéry, *CrystEngComm*, 2014, **16**, 1724–1734; (*b*) K. Molčanov, B. Kojić-Prodić, D. Babić and J. Stare, *CrystEngComm*, 2013, **15**, 135–143; (*c*) K. Molčanov, B. Kojić-Prodić, D. Babić, D. Pajić, N. Novosel and K. Zadro, *CrystEngComm*, 2012, **14**, 7958–7964; (*d*) K. Molčanov, B. Kojić-Prodić, D. Babić, D. Žilić and B. Rakvin, *CrystEngComm*, 2011, **13**, 5170–5178; (*e*) K. Molčanov, I. Sabljić and B. Kojić-Prodić, *CrystEngComm*, 2011, **13**, 4211–4217; (*f*) K. Molčanov, B. Kojić-Prodić and A. Meden, *CrystEngComm*, 2009, **11**, 1407–1415.

16 F. Zhuge, B. Wu, J. Liang, J. Yang, Y. Liu, C. Jia, C. Janiak, N. Tang and X.-J. Yang, *Inorg. Chem.*, 2009, **48**, 10249–10256.

17 (*a*) M. Meot-Ner, *Chem. Rev.*, 2012, **112**, PR22–PR103; (*b*) J. K. Maclaren and C. Janiak, *Inorg. Chim. Acta*, 2012, **389**, 183–190; (*c*) D. Mekhatria, S. Rigolet, C. Janiak, A. Simon-Masseron, M. A. Hasnaoui and A. Benguedach, *Cryst. Growth Des.*, 2011, **11**, 396–404; (*d*) B. M. Drašković, G. A. Bogdanović, M. A. Neelakantan, A.-C. Chamayou, S. Thalamuthu, Y. S. Avadhut, J. Schmedt auf der Günne, S. Banerjee and C. Janiak, *Cryst. Growth Des.*, 2010, **10**, 1665–1676; (*e*) B. Gil-Hernández, H. A. Höppe, J. K. Vieth, J. Sanchiz and C. Janiak, *Chem. Commun.*, 2009, 8270–8272.

18 (*a*) M. B. Andrews and C. L. Cahill, *CrystEngComm*, 2013, **15**, 3082–3086; (*b*) K. Molčanov and B. Kojić-Prodić, *CrystEngComm*, 2010, **12**, 925–939; (*c*) A. Pevec and A. Demšar, *J. Fluorine Chem.*, 2008, **129**, 707–712; (*d*) A. Pevec, M. Tekavec and A. Demšar, *Polyhedron*, 2011, **30**, 549–555.

19 (*a*) A. C. McKinlay, R. E. Morris, P. Horcajada, G. Férey, R. Gref, P. Couvreur and C. Serre, *Angew. Chem., Int. Ed.*, 2010, **49**, 6260–6266; (*b*) P. Horcajada, R. Gref, T. Baati, P. K. Allan, G. Maurin, P. Couvreur, G. Férey, R. E. Morris and C. Serre, *Chem. Rev.*, 2012, **112**, 1232–1268.

20 (*a*) S. W. Jaros, P. Smoleński, M. F. C. G. da Silva, M. Florek, J. Król, Z. Staroniewicz, A. J. L. Pombeiro and A. M. Kirillov, *CrystEngComm*, 2013, **15**, 8060–8064; (*b*) S. R. Miller, P. Horcajada and C. Serre, *CrystEngComm*, 2011, **13**, 1894–1898; (*c*) S. R. Miller, D. Heurtaux, T. Baati, P. Horcajada, J.-M. Grenèche and C. Serre, *Chem. Commun.*, 2010, **46**, 4526–4528.

21 (*a*) F. Semerci, O. Z. Yeşilel, S. Keskin, C. Darcan, M. Taş and H. Dal, *CrystEngComm*, 2013, **15**, 1244–1256; (*b*) H. Eshtiagh-Hosseini, M. Mirzaei, M. Biabani, V. Lippolis, M. Chahkandi and C. Bazzicalupi, *CrystEngComm*, 2013, **15**, 6752–6768; (*c*) M. Mirzaei, H. Eshtiagh-Hosseini, Z. Karrabi, K. Molčanov, E. Eydizadeh, J. T. Mague, A. Bauzá and A. Frontera, *CrystEngComm*, 2014, **16**, 5352–5363; (*d*) G. Hundal, M. S. Hundal, Y. K. Hwang and J. S. Chang, *Cryst. Growth Des.*, 2014, **14**, 172–176; (*e*) A. Husain and C. L. Oliver, *CrystEngComm*, 2014, **16**, 3749–3757; (*f*) T.-W. Tseng, T.-T. Luo, C.-C. Su, H.-H. Hsu, C.-I. Yang and K.-L. Lu, *CrystEngComm*, 2014, **16**, 2626–2633; (*g*) B.-M. Kukovec, G. A. Venter and C. L. Oliver, *Cryst. Growth Des.*, 2012, **12**, 456–465; (*h*) M. A. Sharif and G. R. Najafi, *Acta Chim. Slov.*, 2013, **60**, 138–143; (*i*) L. B. Hamdy, P. R. Raithby, L. H. Thomas and C. C. Wilson, *New J. Chem.*, 2014, **38**, 2135.

22 (*a*) A. T. Çolak, F. Çolak, O. Z. Yeşilel, D. Akduman, F. Yılmaz and M. Tümer, *Inorg. Chim. Acta*, 2010, **363**, 2149–2162; (*b*) E.-J. Gao, M.-C. Zhu, Y. Huang, L. Liu, H.-Y. Liu, F.-C. Liu, S. Ma and C.-Y. Shi, *Eur. J. Med. Chem.*, 2010, **45**, 1034–1041.

23 (*a*) P. Van Der Voort, K. Leus, Y.-Y. Liu, M. Vandichel, V. Van Speybroeck, M. Waroquierb and S. Biswasa, *New J. Chem.*, 2014, **38**, 1853–1867; (*b*) M. Riou-Cavellec, M. Sanselme and

G. Férey, *J. Mater. Chem.*, 2000, **10**, 745–748; (*c*) K. Barthelet, J. Marrot, D. Riou and G. Férey, *Angew. Chem., Int. Ed.*, 2002, **41**, 281–284.

24 (*a*) G. R. Willsky, L.-H. Chi, M. Godzala III, P. J. Kostyniak, J. J. Smee, A. M. Trujillo, J. A. Alfano, W. Ding, Z. Hu and D. C. Crans, *Coord. Chem. Rev.*, 2011, **255**, 2258–2269; (*b*) T. Kiss, T. Jakusch, B. Gyurcsik, A. Lakatos, É. A. Enyedy and É. Sija, *Coord. Chem. Rev.*, 2012, **256**, 125–132; (*c*) H. Sakurai, Y. Yoshikawa and H. Yasui, *Chem. Soc. Rev.*, 2008, **37**, 2383–2392; (*d*) T. Koleša-Dobravc, E. Lodyga-Chruscinska, M. Symonowicz, D. Sanna, A. Meden, F. Perdih and E. Garribba, *Inorg. Chem.*, 2014, **53**, 7960–7976; (*e*) T. Koleša-Dobravc, A. Meden and F. Perdih, *Monatsh. Chem.*, 2014, **145**, 1263–1275.

25 V. Stilinović, D.-K. Bučar, I. Halasz and E. Meštrović, *New J. Chem.*, 2013, **37**, 619–623.

26 G. Labbé, A. P. Krismanich, S. de Groot, T. Rasmusson, M. Shang, M. D. R. Brown, G. I. Dmitrienko and J. G. Guillemette, *J. Inorg. Biochem.*, 2012, **112**, 49–58.

27 W. Rasshofer, W. M. Mueller and F. Voegtle, *Chem. Ber.*, 1979, **112**, 2095–2119.

28 Z. Otwinowski and W. Minor, *Methods Enzymol.*, 1997, **276**, 307–326.

29 *CrysAlis PRO*, Agilent Technologies, Yarnton, England, 2011.

30 G. M. Sheldrick, *Acta Crystallogr., Sect. A: Found. Crystallogr.*, 2008, **64**, 112–122.

31 A. Altomare, M. C. Burla, M. Camalli, G. Cascarano, C. Giacovazzo, A. Guagliardi, A. G. G. Moliterni, G. Polidori and R. Spagna, *J. Appl. Crystallogr.*, 1999, **32**, 115–119.

32 M. C. Burla, R. Caliandro, M. Camalli, B. Carrozzini, G. L. Cascarano, L. De Caro, C. Giacovazzo, G. Polidori and R. Spagna, *J. Appl. Crystallogr.*, 2005, **38**, 381–388.

33 B. S. Parajón-Costa, O. E. Piro, R. Pis-Diez, E. E. Castellano and A. C. González-Baró, *Polyhedron*, 2006, **25**, 2920–2928.

34 K. Nakamoto, *Infrared and Raman Spectra of Inorganic and Coordination Compounds: Theory and Applications in Inorganic Chemistry*, John Wiley & Sons, New York, 1997.

35 H. Aghabozorg and E. Sadr-khanlou, *Acta Crystallogr., Sect. E: Struct. Rep. Online*, 2007, **63**, m1753.

36 A. W. Addison, T. N. Rao, J. Reedijk, J. van Rijn and G. C. Verschoor, *J. Chem. Soc., Dalton Trans.*, 1984, 1349–1356.

37 (*a*) J. Bernstein, R. E. Davis, L. Shimoni and N.-L. Chang, *Angew. Chem., Int. Ed.*, 1995, **34**, 1555–1573; (*b*) M. C. Etter, *Acc. Chem. Res.*, 1990, **23**, 120–126.

38 (*a*) T. Dorn, A.-C. Chamayou and C. Janiak, *New J. Chem.*, 2006, **30**, 156–167; (*b*) J. K. Maclaren, J. Sanchiz, P. Gili and C. Janiak, *New J. Chem.*, 2012, **36**, 1596–1609; (*c*) M. Enamullah, V. Vasylyeva and C. Janiak, *Inorg. Chim. Acta*, 2013, **408**, 109–119.